JB
Journals.ASM.org

Characterization of a *mazEF* Toxin-Antitoxin Homologue from *Staphylococcus equorum*

Christopher F. Schuster,[a] Jung-Ho Park,[b]* Marcel Prax,[a] Alexander Herbig,[c] Kay Nieselt,[c] Ralf Rosenstein,[a] Masayori Inouye,[b] Ralph Bertram[a]

Department of Microbial Genetics, Interfaculty Institute of Microbiology and Infection Medicine Tübingen (IMIT), Faculty of Science, University of Tübingen, Tübingen, Germany[a]; Integrative Transcriptomics, Center for Bioinformatics, University of Tübingen, Tübingen, Germany[c]; Center for Advanced Biotechnology and Medicine (CABM), Department of Biochemistry, Robert Wood Johnson Medical School, Piscataway, New Jersey, USA[b]

Toxin-antitoxin (TA) systems encoded in prokaryotic genomes fall into five types, typically composed of two distinct small molecules, an endotoxic protein and a *cis*-encoded antitoxin of ribonucleic or proteinaceous nature. *In silico* analysis revealed seven putative type I and three putative type II TA systems in the genome of the nonpathogenic species strain *Staphylococcus equorum* SE3. Among these, a MazEF system orthologue termed $MazEF_{seq}$ was further characterized. 5′ rapid amplification of cDNA ends (RACE) revealed the expression and the transcriptional start site of $mazE_{seq}$, indicating an immediately upstream promoter. Heterologous expression of the putative toxin-encoding $mazF_{seq}$ gene imposed growth cessation but not cell death on *Escherichia coli*. *In vivo* and *in vitro*, $MazF_{seq}$ was shown to cleave at UACAU motifs, which are remarkably abundant in a number of putative metabolic and regulatory *S. equorum* gene transcripts. Specific interaction between $MazF_{seq}$ and the putative cognate antitoxin $MazE_{seq}$ was demonstrated by bacterial two-hybrid analyses. These data strongly suggest that $MazEF_{seq}$ represents the first characterized TA system in a nonpathogenic *Staphylococcus* species and indicate that MazEF modules in staphylococci may also control processes beyond pathogenicity.

Toxin-antitoxin (TA) systems are small episomally or chromosomally encoded genetic modules found in bacteria or archaea (1). TA systems typically consist of a small and stable toxic protein that can interfere with vital cellular functions and an unstable antitoxin, capable of inhibiting toxin activity (2). Depending on the biochemical nature and mode of action of the antitoxin, five classes can be distinguished. Type I TA systems possess an RNA antitoxin that posttranscriptionally inhibits toxin activity via antisense regulation. TA systems of types II, IV, and V contain a small proteinaceous antitoxin that can render the toxin inactive either by protein-protein interaction, by cleavage of toxin mRNA, or by binding to the toxin's target structure. Type III TA systems (3) are characterized by an RNA antitoxin modulating toxicity in a posttranslational fashion (4). TA systems of types III, IV, and V have so far been characterized in only one instance each (5–7), but orthologues of type I, type II, and supposedly also type III representatives are widespread among plasmids and chromosomes of prokaryotes (3, 8). According to toxin sequence homology, at least 10 families of type II TA systems can be distinguished (4, 9–11). The genome of the notorious pathogen *Staphylococcus aureus* possibly bears a number of type I TA systems, from which one candidate has recently been characterized (12). Three type II TA systems, $MazEF_{sa}$, YefM-YoeB-sa1, and YefM-YoeB-sa2, have been validated, and all of them encode endoribonucleases. The sequence-specific RNA cleavage activity of $MazF_{sa}$ can be inhibited by its cognate antitoxin $MazE_{sa}$, which, in turn, is subject to degradation by the ClpPC proteolytic system (13). Transcriptionally, the $mazEF_{sa}$ genes are downregulated by the alternative sigma factor σ^B and induced by the global regulator *sarA* (14), in contrast to *Escherichia coli*, where *mazEF* is negatively autoregulated (15). Overexpression of $mazF_{sa}$ was found to result in a growth defect in *S. aureus* (16, 17, 19). Unlike $MazF_{sa}$, endoribonuclease activity of YoeB-sa1 and YoeB-sa2 is stimulated by ribosome association to cleave mRNAs adjacent to the start codon (20). Expression of both *yefM-yoeB*-sa paralogues is transcriptionally autoregulated but is also increased by certain antibiotic stresses (14). Research on TA systems in staphylococci has to date been confined to *S. aureus*, neglecting at least 41 further species of this genus (21). Staphylococci form a distinct monophyletic group (which can further be divided into different species and cluster groups), also comprising a number of nonpathogenic species (22), such as *Staphylococcus equorum*, a member of the *Staphylococcus saprophyticus* cluster and thus relatively distantly related to *S. aureus*. *S. equorum* was originally isolated from the skin of healthy horses (23) and was later also found on the surface of red-smear cheese. Some strains are able to inhibit the growth of the food-borne pathogen *Listeria monocytogenes* by producing the macrocyclic, nonribosomally synthesized peptide antibiotic micrococcin P_1 (24, 25). It has therefore been suggested to use such *S. equorum* strains in cheese starter cultures to prevent growth of *L. monocytogenes* and other undesired bacteria. A genome-sequencing program for strain *S. equorum* SE3 has recently been started (F. Götz and R. Rosenstein, unpublished data). In this study, we performed extensive *in silico* screening for TA systems in the *S. equorum* SE3 raw, partially assembled sequencing data, revealing a number of putative type I

Received 14 March 2012 **Accepted** 21 October 2012
Published ahead of print 26 October 2012
Address correspondence to Ralph Bertram, ralph.bertram@uni-tuebingen.de.
* Present address: Jung-Ho Park, Bio-Evaluation Center, Korea Research Institute of Bioscience and Biotechnology, Ochang-eup, Cheongwon-gun, Chungcheong-do, Republic of Korea.
Supplemental material for this article may be found at http://dx.doi.org/10.1128/JB.00400-12.

doi:10.1128/JB.00400-12

and type II TA systems. Among these, a gene pair dubbed *mazEF*$_{seq}$ was genetically and biochemically characterized and yielded strong evidence for a first characterized functional TA system encoded in the *S. equorum* genome. We determined the transcriptional starting point of the *mazEF*$_{seq}$ locus and provide evidence for a toxic effect of *mazF*$_{seq}$ expression and for *in vivo* interaction of MazF$_{seq}$ and MazE$_{seq}$ in *E. coli*. It is shown that the purified putative toxin endolytically cleaves RNA in a sequence-specific manner, as it also does upon heterologous expression *in vivo*. Finally, we identified coding sequences that might posttranscriptionally be controlled by MazF$_{seq}$-dependent cleavage due to unusually high relative abundances of respective target sites.

MATERIALS AND METHODS

Bioinformatical analysis. Access to the raw, partially assembled genome sequence of *Staphylococcus equorum* SE3 was kindly provided by F. Götz. Initially, a local BLAST protein database consisting of putative type I TA system toxins described by Fozo et al. (26) was created. Manual BLASTX searches were done against the *S. equorum* raw genome to identify homologues of type I TA toxin components. Furthermore, the antitoxin RNAs of putative type I TA systems were analyzed to assess their structure and RNA-RNA interaction potential. The program RNAz (27, 28) was used to predict conserved secondary structures between the homologous RNAs. The input alignment for RNAz was calculated using ClustalW (29). For the prediction of RNA-RNA interactions, the program IntaRNA (30, 31) was applied. In addition, a prediction of promoter regions, which is based on the detection of destabilized regions (32), was performed using nocoRNAc (33).

In silico screenings for type II TA systems were conducted using the web-based search tools RASTA Bacteria (34) and TADB (35). Obtained sequences were aligned using ClustalW (29) and viewed in Jalview (36) or BioEdit (37). For all programs, standard parameters were used.

Fine chemicals, nucleic acids, and enzymes. Chemicals were from Carl Roth (Karlsruhe, Germany), Sigma-Aldrich (St. Louis, MO), Fisher Scientific (Fair Lawn, NJ), and J. T. Baker (Phillipsburg, NJ) at the highest purities available. Enzymes for DNA restriction and modification were purchased from NEB (Ipswich, MA), Fermentas (St. Leon-Rot, Germany), and TaKaRa Bio Inc. (Shiga, Japan). DNA polymerases were obtained from Genaxxon (Ulm, Germany) and Agilent Technologies (La Jolla, CA). Avian myeloblastosis virus reverse transcriptase (AMV RT), MS2 phage RNA, and RNase inhibitor for primer extension were purchased from Roche (Indianapolis, IN). For 5′ RACE (rapid amplification of cDNA ends) analysis, Ambion SUPERase-In, Ambion diethyl pyrocarbonate (DEPC)-treated double-distilled water (ddH_2O), Ambion THE RNA storage solution, and the Topo TA cloning kit for sequencing with One Shot chemically competent T10 *E. coli* cells were purchased from Life Technologies (Darmstadt, Germany); Roti-Aqua-P/C/I (phenol-chloroform-isoamyl alcohol, 25:24:1, pH 4.5 to 5) was purchased from Carl Roth GmbH + Co. KG (Karlsruhe, Germany); T4 RNA ligase was purchased from NEB (Ipswich, MA); tobacco acid phosphatase (TAP) was purchased from Epicentre (Madison, WI); and the first-strand cDNA synthesis kit for reverse transcription-PCR (RT-PCR) was purchased from Roche (Mannheim, Germany). Protein and DNA molecular weight markers and loading dyes were bought from NEB (Ipswich, MA), Invitrogen/Life Technologies (Carlsbad, CA), Promega (Madison, WI), and Fermentas (St. Leon-Rot, Germany). The Thermo Sequenase fluorescently labeled primer cycle sequencing kit with 7-deaza-dGTP was acquired from GE Healthcare (Freiburg, Germany). Isopropyl-β-D-thiogalactopyranoside (IPTG) was ordered from Merck (Darmstadt, Germany), and anhydrotetracycline (ATc) was ordered from Acros Organics (Geel, Belgium). Lysostaphin was acquired from Dr. Petry Genmedics (Reutlingen, Germany). Nickel-nitrilotriacetic acid (Ni-NTA) resin was purchased from Qiagen (Hilden, Germany). Synthetic DNA and RNA oligonucleotides were ordered from Biomers (Ulm, Germany) and Integrated DNA Technologies (Coralville, IA).

Bacterial strains, plasmids, and growth conditions. The *E. coli* strains BL21(DE3) (38), DH5α (39), BW25113 (40), and BTH101 (41) (Euromedex, Souffelweyersheim, France), as well as *S. equorum* SE3 (kindly provided by F. Götz), were used in this study (Table 1). *E. coli* cells were grown either in LB or, whenever sugar-sensitive inducible plasmids were used, in M9 minimal medium (44) supplemented with 0.2% (wt/vol) thiamine, 0.2% (wt/vol) Casamino Acids (CAA), and either 0.4% (wt/vol) glucose or 0.2% (vol/vol) glycerol as a carbon source. During the BACTH bacterial two-hybrid experiments (see below), cells were grown on LB agar plates supplemented with X-Gal (5-bromo-4-chloro-3-indolyl-β-D-galactopyranoside) and IPTG (both from Carl Roth, Karlsruhe, Germany) at final concentrations of 40 μg/ml or 0.5 mM, respectively. *S. equorum* was grown in basic medium (BM) (45). All cultures were grown with shaking (150 rpm) in baffle flasks at 37°C with aeration. Antibiotics were used where appropriate at the following concentrations: 100 μg/ml ampicillin, 25 μg/ml chloramphenicol, and 50 μg/ml kanamycin.

Molecular cloning and isolation of nucleic acids. In general, cloning was carried out using standard protocols. *E. coli* cells were made chemically competent by RbCl treatment (46). Plasmids and DNA fragments were isolated or purified using standard kits from Sigma-Aldrich (Munich, Germany), Peqlab (Erlangen, Germany), and Qiagen (Hilden, Germany) according to the manufacturers' protocols. Genomic DNA of staphylococci was obtained either by breaking cells with lysostaphin (15 μg/ml for 90 min) and $NaClO_4$ treatment and chloroform-isoamyl alcohol extraction as described previously (47, 48) or by using the *InstaGene kit* (Bio-Rad, Munich, Germany). The nucleotide sequence of the *S. equorum mazEF*$_{seq}$ locus can be found under the GenBank accession number KC020193. Sequencing of cloned products was done at GATC (Constance, Germany) and Macrogen Corp. (New York, NY), and results were confirmed using Lasergene SeqMan (DNAStar, Madison, WI).

Construction and growth analysis of *E. coli* DH5α(pASK-IBA3 *mazF*$_{seq}$). *mazF*$_{seq}$, including its native ribosome-binding site (RBS), was PCR amplified from *S. equorum* SE3 genomic DNA (GenBank accession number KC020193) using the primers mazF_f and mazF_r (all oligonucleotides are listed in Table S1 in the supplemental material). The PCR product was digested with BglII and NcoI and ligated with the ATc-inducible vector pASK-IBA3 cut with NcoI and BamHI, yielding pASK-IBA3-*mazF*$_{seq}$, which was used to transform *E. coli* DH5α. Resulting strains carrying pASK-IBA3 with or without *mazF*$_{seq}$ were grown overnight in LB, and cultures from both strains were used to inoculate two flasks containing 17 ml of LB each to an optical density at 578 nm (OD_{578}) of 0.07. Cells were cultivated with shaking at 37°C, and 60 min later, ATc (0.4 μM final concentration) was added to one flask of each strain. Growth was monitored on an hourly basis by determining both OD_{578} values (measured as 10-fold or 20-fold dilutions, where necessary) and CFU counts. To this end, samples were 10-fold serially diluted from 10^0 to 10^{-7} in sterile saline solution (0.85% [wt/vol] NaCl) and plated on LB plates containing ampicillin. After 14 to 16 h of incubation at 37°C, the numbers of colonies were counted.

BACTH two-hybrid analysis of MazE$_{seq}$-MazF$_{seq}$ interaction *in vivo*. The bacterial adenylate cyclase-based two-hybrid system (BACTH; Euromedex, Souffelweyersheim, France) functions by fusing two putative binding partners to the *Bordetella pertussis* adenylate cyclase (CyaA) fragments T18 and T25. These form an active enzyme only when in close proximity, providing evidence for interaction of the fused proteins. The cyclic AMP (cAMP)-dependent activation of lactose-utilizing genes is visualized by blue colonies on X-Gal-containing medium. We cloned *mazE*$_{seq}$ in two ways to the T18-encoding fragment, to obtain N- and C-terminal translational fusions using the high-copy-number BACTH vectors pUT18 (*mazE*$_{seq}$ N terminally fused) and pUT18C (C-terminal fusion). Products amplified by PCR using the primers mazE_bacth_f and mazE_bacth_r were cloned with the restriction enzymes BamHI and XmaI. Similarly, *mazF*$_{seq}$ was cloned in frame with the T25 open reading frame

TABLE 1 Strains and plasmids used in this study

Strain or plasmid	Description or information	Reference and/or source
Strains		
E. coli		
BL21(DE3)	F$^-$ *ompT gal dcm lon hsdS*$_B$(r_B^- m_B^-) λ(DE3 [*lacI lacUV5-T7* gene 1 *ind1 sam7 nin5*])	38
DH5α	F$^-$ *endA1 glnV44 thi-1 recA1 relA1 gyrA96 deoR nupG* ϕ80d*lacZ*ΔM15 Δ(*lacZYA-argF*)*U169 hsdR17*(r_K^- m_K^+) λ$^-$	39
Top10	F$^-$ *mcrA* Δ(*mrr-hsdRMS-mcrBC*) ϕ80*lacZ*ΔM15 Δ*lacX74 recA1 araD139* Δ(*ara-leu*)*7697 galU galK rpsL* (Str^r) *endA1 nupG* λ$^-$	Invitrogen/Life Technologies, Carlsbad, CA
BTH101	F$^-$ *cya-99 araD139 galE15 galK16 rpsL1* (Str^r) *hsdR2 mcrA1 mcrB1*	41; Euromedex, Souffelweyersheim, France
BW25113	*rrnB3* Δ*lacZ4787 hsdR514* Δ(*araBAD*)*567* Δ(*rhaBAD*)*568 rph-1*	40
S. equorum SE3	Isolated from red-rind cheese	German Federal Dairy Research Centre, Max Rubner Institute, Kiel, Germany
Plasmids		
pASK-IBA3	*bla*, ATc-inducible promoter	IBA-GmbH, Göttingen, Germany
pASK-IBA3 *mazF*$_{seq}$	*mazF*$_{seq}$ cloned downstream of the ATc-inducible promoter	This study
pBAD33	*cat*, arabinose-inducible promoter	42
pBAD33 SD *mazF*$_{seq}$	*mazF*$_{seq}$ cloned downstream of an arabinose-inducible promoter with a synthetic *E. coli* Shine-Dalgarno sequence	This study
pColdIII	*bla*, IPTG- and cold shock-inducible promoter	43; TaKaRa Bio Inc., Shiga, Japan
pColdIII *mazF*$_{seq}$	*mazF*$_{seq}$ cloned downstream of the IPTG- and cold shock-inducible promoter	This study
pUT18	*bla*, MCS[a] in N terminus of T18 fragment	41; Euromedex, Souffelweyersheim, France
pUT18C	*bla*, MCS in C terminus of T18 fragment	41; Euromedex, Souffelweyersheim, France
pUT18C-*zip*	Derivative, *bla*, leucine zipper C terminally fused to T18 fragment	41; Euromedex, Souffelweyersheim, France
pKT25	*aphAIII*, MCS in C terminus of T25 fragment	41; Euromedex, Souffelweyersheim, France
pKNT25	*aphAIII*, MCS in N terminus of T25 fragment	41; Euromedex, Souffelweyersheim, France
pKT25-*zip*	Derivative, *aphAIII*, leucine zipper C terminally fused to T25 fragment	41; Euromedex, Souffelweyersheim, France
pUT18-*mazE*	Derivative, *bla*, *mazE*$_{seq}$ N terminally fused to T18 fragment	This study
pUT18C-*mazE*	Derivative, *bla*, *mazE*$_{seq}$ C terminally fused to T18 fragment	This study
pUT18-*yefM1*	Derivative, *bla*, *yefM1*$_{seq}$ N terminally fused to T18 fragment	This study
pUT18C-*yefM1*	Derivative, *bla*, *yefM1*$_{seq}$ C terminally fused to T18 fragment	This study
pKT25-*mazF*	Derivative, *aphAIII*, *mazF*$_{seq}$, C terminally fused to T25 fragment	This study
pKT25-*yoeB1*	Derivative, *aphAIII*, *yoeB*-seq1, C terminally fused to T25 fragment	

[a] MCS, multiple-cloning site.

(ORF) into the low-copy-number BACTH vector pKT25 (C-terminal fusion) using the primers mazF_bacth_f and mazF_bacth_r and restriction enzymes as described above. Constructs were confirmed by sequencing, and the pUT18-, pUT18C-, and pKT25-derived vectors were used to consecutively transform strain *E. coli* BTH101. Single colonies of cells containing both plasmids (one each of the pUT and of the pKT series) were streaked onto LB–X-Gal–IPTG plates to provide evidence for protein-protein interaction. As negative controls, strains that harbor a plasmid containing the T18 fragment alone with either a plasmid containing only the T25 fragment or the T25 fragment translationally fused with a leucine zipper component (from N to C terminus, T25-zip) were used. In addition, the genes *yefM*-seq1 and *yoeB*-seq1 from *S. equorum* were PCR amplified using the primer pairs yefM1_bacth_f and yefM1_bacth_r or yoeB1_bacth_f and yoeB1_bacth_f and cloned via BamHI/XmaI in frame with the adenylate cyclase-encoding fragments into the vector(s) pUT18/pUT18C or pKT25, respectively. These *yefM*-seq1 and *yoeB*-seq1 constructs were used to transform cells containing the appropriate corresponding *mazE*$_{seq}$ or *mazF*$_{seq}$ constructs to obtain additional negative controls. None of these showed coloring on LB–X-Gal–IPTG agar plates, whereas the interaction of the two leucine zipper components (T18-zip and T25-zip) of the positive control was clearly visible as a blue coloration.

Overexpression and purification of (His)$_6$-tagged MazF$_{seq}$. *mazF*$_{seq}$ was PCR amplified from genomic DNA using primers mazFhis_r and mazFhis_f, introducing codons for a C-terminally fused (His)$_6$ tag, and the product was cloned into the IPTG- and cold shock-inducible vector pColdIII via NdeI and BamHI. *E. coli* BL21(DE3) carrying the resulting vector pColdIII *mazF*$_{seq}$ was grown at 37°C in M9 medium supplemented with Casamino Acids and glucose to an OD_{600} of 0.5. Cultures were then induced by 5-min incubation on ice and IPTG (0.5 mM final concentration), grown subsequently at 15°C, and lysed after 24 h using a French press (Thermo Scientific, Waltham, MA). MazF$_{seq}$-(His)$_6$ was purified using a Ni-NTA resin according to the manufacturer's protocol (Qiagen, Valencia, CA), dialyzed twice (20 mM phosphate buffer, 5 mM dithiothreitol [DTT], 100 mM NaCl, 0.5 mM EDTA), and stored in this buffer at −20°C in aliquots.

Elucidation of MazF$_{seq}$ target specificity by primer extension analysis. *In vitro* primer extension experiments were done as described previously (19). Briefly, 800 ng of MS2 phage RNA (NCBI accession number NC_001417.2, purchased from Roche, Indianapolis, IN) was incubated with 1 μg of purified MazF$_{seq}$-(His)$_6$ in 10 mM Tris-HCl (pH 7.8), also containing 0.5 μl RNase inhibitor (Roche, Indianapolis, IN) and 32 μg CspA for 30 min at 37°C, in a total reaction volume of 10 μl. CspA, a cold shock protein and RNA chaperone from *E. coli*, was purified as previously described (49). Prior to use, primers were 5′ labeled using a T4 polynucleotide kinase and [γ-^{32}P]ATP. Primer extension reactions were carried out with added MS2 RNA fragments, AMV RT, and labeled primers for 1 h at 47°C. The extension reaction was terminated by the addition of 6 μl of stop solution 1 (95% formamide, 20 mM EDTA, 0.05% bromophenol

blue, and 0.05% xylene cyanol EF), incubation for 2 min at 95°C, and storage on ice for 5 min. After being heated to 90°C for 5 min, samples were electrophoresed on a 6% polyacrylamide gel with 8 M urea, which was subsequently dried for 2 h in a gel vacuum dryer before an X-ray film (Kodak, Rochester, NY) was exposed for 20 to 48 h.

In vivo primer extension assays were performed according to the literature (20, 50), but instead of using ^{32}P labeling, primers were ordered with a DY-681 (Dyomics, Jena, Germany) infrared dye modification at the 5′ end. Plasmid pBAD33 SD $mazF_{seq}$ was constructed by cloning PCR-amplified $mazF_{seq}$ (primers mazF_BAD_f and mazF_BAD_r) into pBAD33 via SacI and XbaI. *E. coli* BW25113 cells containing pBAD33 SD $mazF_{seq}$ or the empty pBAD33 vector were grown in 250-ml flasks containing 100 ml BM to an OD_{578} of 0.6. The cells were then split, and to one flask of each construct, arabinose was added to a final concentration of 0.2% (wt/vol). After 40 min, 12 ml of culture from each flask was harvested and the cells were broken by treatment with glass beads (Roth, Karlsruhe, Germany) and a tissue lyser (Thermo Savant; FastPrep FP120 Bio101) twice for 20 s. Total RNA was extracted from the lysate using TRIzol (Ambion, Life Technologies, Darmstadt, Germany) according to the manufacturer's protocol, the RNA pellets were dissolved in THE RNA storage solution (Ambion, Life Technologies, Darmstadt, Germany), and the concentration was determined by NanoDrop measurement. Reverse transcription was conducted in the presence of 16 μg total RNA, 1 pmol DY-681-labeled primer (OmpF_ec or TufA_ec), 10 mmol deoxynucleoside triphosphates (dNTPs), 10 U AMV RT (Roche), 1× AMV RT buffer, and 4 U of SUPERase-In RNase inhibitor in a total volume of 10 μl for 60 min at 47°C and stopped by the addition of 6 μl stop solution 2 (95% formamide, 10 mM EDTA, 0.05% bromophenol blue). Sequencing ladders were generated from genomic DNA prepared from *E. coli* BW25113 pBAD33 cells using the Thermo Sequenase fluorescently labeled primer cycle sequencing kit with 7-deaza-dGTP (GE Healthcare, Freiburg, Germany) and the primers OmpF_ec and TufA_ec. All samples were heated for 2 min at 95°C and then loaded onto a 25 cm 8M urea, 10% polyacrylamide gel and run on a Li-Cor Long ReadIR 4200 system (Lincoln, NE) using the IRD700 channel according to the manufacturer's recommendations.

For RNA oligonucleotide digestion tests, γ-^{32}P-labeled fragments were subjected either to digestion by purified $MazF_{seq}$-$(His)_6$ or to chemical hydrolysis, to provide a molecular weight standard ladder for electrophoresis. In a total volume of 10 μl, 0.5 μl RNase inhibitor, 0.25 μg $MazF_{seq}$-$(His)_6$, 1 μl Tris-HCl (pH 7.8, 100 mM), and 0.5 μl radioactively labeled primer (10 pmol/μl) were mixed and incubated for 30 min at 37°C for enzymatic cleavage by $MazF_{seq}$-$(His)_6$. The reaction was stopped as before. A nucleotide ladder was created by mixing 2 μl of labeled RNA with 1 μl NaOH (1 M) and 7 μl DEPC-treated H_2O and incubating the mixture for 1 min at 75°C followed by terminating the reaction with 40 μl stop buffer. The samples were loaded onto a 20% SDS gel with 8 M urea and further processed as described above.

Transcription start site determination by 5′ RACE. An *S. equorum* culture was grown in BM to an OD_{578} of 1.4, and the RNA was isolated as described above (*in vivo* primer extension). 5′ RACE was essentially done as described before (51). Specifically, 7.5 μg of total RNA was incubated with 12.5 U of tobacco acid pyrophosphatase (TAP), 20 U of SUPERase-In (Ambion, Life Technologies, Darmstadt, Germany), and 1× TAP buffer for 1 h at 37°C. This modified RNA was extracted with acidic P/C/I solution, ethanol precipitated, dissolved in 55 μl DEPC-treated ddH_2O, and incubated with 500 pmol of an RNA adapter fragment (see Table S1 in the supplemental material) at 95°C for 5 min. Ligation of cellular RNA molecules with the RNA adapter was done for 90 min at 16°C with 50 U of T4 RNA ligase I, 20 U of SUPERase-In, 1× T4 RNA ligase buffer, 1 mM ATP, and 1 mg/ml bovine serum albumin (BSA) in a total volume of 80 μl. The ligated RNA was phenol-chloroform extracted and ethanol precipitated as before and resuspended in 10 μl DEPC-treated ddH_2O. Five microliters was used for reverse transcription by using the Roche first-strand cDNA synthesis kit for RT-PCR (containing AMV RT) with a primer specific for $mazE_{seq}$ (mazE-RACE-outer) in a total volume of 20 μl. One microliter of 10-fold-diluted cDNA was PCR amplified using 1 μM (each) primers specific for the adapter (RACE-PCR) and for $mazE_{seq}$ (mazE-RACE-inner), 1 mM dNTPs, 1× *Taq* buffer E, and 5 U *Taq* polymerase (Genaxxon, Ulm, Germany) in a 50-μl reaction mixture. Amplification of cDNA was confirmed on a 2% agarose gel, and 2 μl of the PCR product was used for ligase- and restriction-independent TOPO cloning followed by transformation of One Shot chemically competent *E. coli* Top10 cells (Invitrogen/Life Technologies). Sequencing of the resulting plasmids allowed determination of the transcriptional start site of $mazEF_{seq}$.

Analysis of TACAT sequence abundance in the *S. equorum* SE3 genome. A screen for TACAT motifs in coding sequences (CDSs) of the *S. equorum* SE3 genome, including an assessment of stochastic or cumulative occurrence, was performed as described previously (19, 52). Briefly, the probability P of a CDS containing K (actual number) or fewer TACAT sites is dependent on the base composition and length (L) and was calculated as follows:

$$P = \sum_{i=0}^{K} p^i (1 - p)^{L-4-i} \frac{(L-4)!}{i!(L-4-i)!}$$

The expected number of TACAT sites is $p(L-4)$ where p, the probability of the pentad sequence occurring in a CDS stochastically, is $p = (\%\text{ of A})^2(\%\text{ of T})^2(\%\text{ of C})^2$. The complete set of 2,581 possible CDSs of *S. equorum* SE3 was exported from an automatically annotated data set using GenDB (53) and passed on to a custom Perl script (the source code is available upon request) calculating P for each CDS and sorting the results in a descending order.

RESULTS AND DISCUSSION

***In silico* analysis indicates several putative type I and type II TA systems in the genome of *Staphylococcus equorum*.** In this study, we were interested in mining the genome of the nonpathogenic, food industry-relevant bacterium *S. equorum* SE3 for putative TA systems, for two main reasons. First, it has been proposed that the abundance of TA systems may be higher in free-living organisms than in host-associated species (8), which would suggest a greater number of such systems in *S. equorum* than in *S. aureus*. Second, one of the TA systems of *S. aureus* was suggested to regulate pathogenicity factors (19), which raises the question whether nonpathogenic staphylococci also possess TA systems and, if so, what their functions might be. In order to identify putative type I TA systems in the raw genome of *S. equorum* SE3, we first conducted manual BLAST searches. Using the putative *S. saprophyticus* type I toxin Fst described by Fozo et al. (26) as a query revealed five possible homologues in *S. equorum* (Fig. 1). Respective systems have previously been suggested to reside on a number of other staphylococcal plasmids and chromosomes (54, 55) but have, with one recent exception (12), not been characterized yet. To assess if the putative antitoxin RNAs of these systems may be transcribed, we performed an *in silico* prediction of promoters by the detection of destabilized regions (33). For three of the five systems, a region with low stability was detected, which complements the presence of −10 and −35 box motifs (Fig. 1). The putative antitoxin RNAs do not overlap the coding sequence of the assumed toxin. Therefore, we performed an *in silico* RNA-RNA interaction prediction between the antitoxin RNAs and the toxin mRNAs. For all five pairs of RNAs, a stable interaction was predicted with free energy values ranging from −16.6 to −23.5 kcal/mol (see Table S2 in the supplemental material). In all cases, the predicted interaction site partly covers the putative ribosome-binding site of the toxin mRNA, providing evidence for a possible regulatory role of the candidate antitoxin RNA. In addition, two possible TxpA/RatA type I TA systems were identified, sharing distinct features with

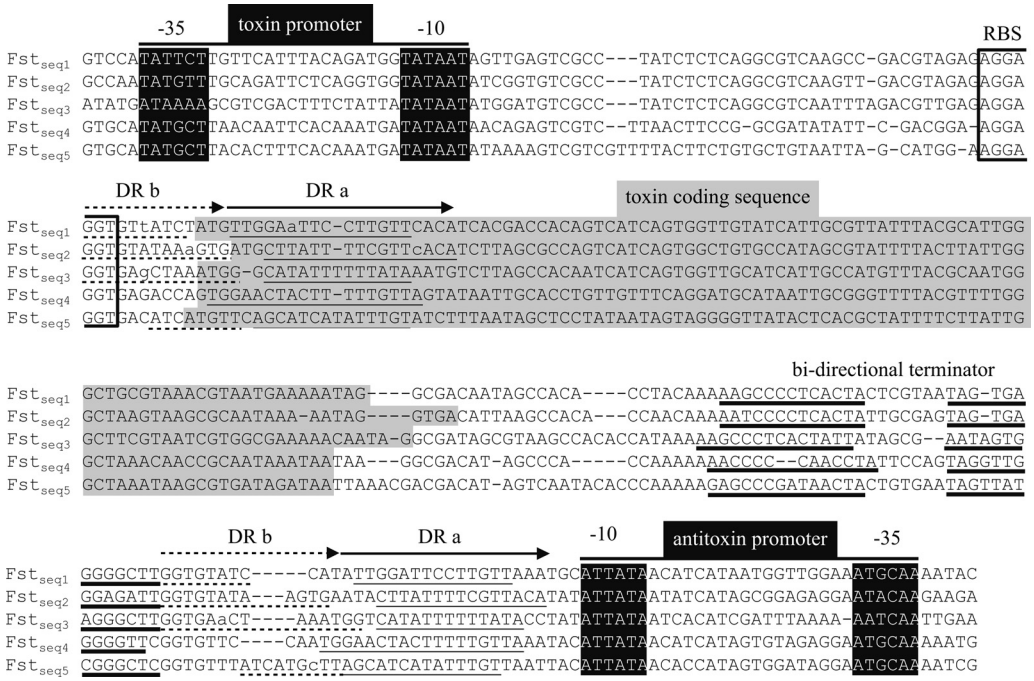

FIG 1 Five different putative type I Fst TA systems from *S. equorum* discovered *in silico*, aligned with ClustalW using manual adjustments similar to those in the work of Jensen et al. (57). Promoter elements are indicated by black shading, the RBS is indicated by a black frame, direct repeats "b" (DR b) are indicated by dashed lines and arrows, direct repeats "a" (DR a) are indicated by solid lines and arrows, the toxin coding region is indicated by gray shading, and bidirectional terminators are indicated by thick black underlining.

putative staphylococcal systems (26). To collect further evidence that the candidate antitoxin RNAs of these systems are functional, we created a ClustalW sequence alignment of the two antitoxin RNAs with the RatA homologue in *S. aureus* (56). According to a prediction by the program RNAz (27), the aligned RNAs contain a stable conserved secondary structure (classifier *P* value, 0.99). This suggests that the two putative antitoxin RNAs identified in *S. equorum* carry out a similar function. Manual BLAST searches for the two representatives of type IV and type V TA systems YeeU-CbtA (6) and GhoST (7) yielded no apparent homologues in *S. equorum*.

For the revelation of putative type II TA systems in the *S. equorum* SE3 genome, the publicly accessible online tools RASTA Bacteria (34) and TADB (35) were used. This approach yielded three candidate loci bearing two distinct putative *yefM-yoeB* systems (Fig. 2) and an apparent *mazEF* orthologue (see below), which reflects the complete set of validated type II TA systems in *S. aureus* (16, 19, 20). Thus, we identified a total of 10 putative TA systems in the *S. equorum* SE3 genome (summarized in Table 2), seven of which belonged to type I and three to type II TA systems. The two putative *yefM-yoeB* paralogues are clearly homologous to the *yefM-yoeB*-sa1 and -sa2 systems from *S. aureus* (20), and the

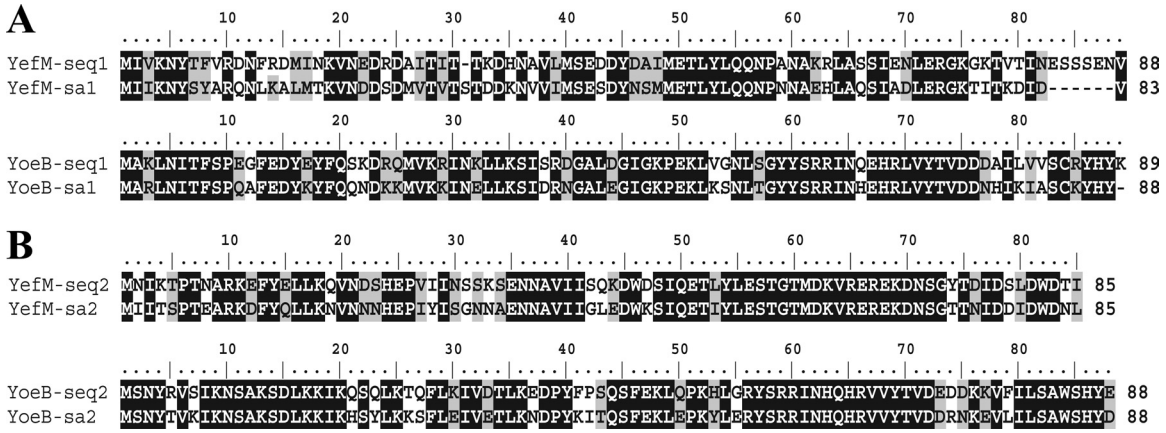

FIG 2 Alignment of YefM-YoeB-sa1 homologues (SA2195 and SA2196) (A) and YefM-YoeB-sa2 homologues (SA2245 and SA2246) (B) from *S. aureus* (sa) N315 with their *S. equorum* (seq) SE3 homologues. Sequences were aligned using MAFFT (63), and residues were shaded according to their BLOSUM62 score in BioEdit (37).

TABLE 2 Identities and similarities of putative *Staphylococcus equorum* SE3 TA systems[f]

Putative TA system	% identity	% similarity	pI value	Size (amino acids)
Type I				
Fst_{seq1} (T)	59	66[a]	9.90	31
Fst_{seq2} (T)	87	93[a]	10.33	31
Fst_{seq3} (T)	48	66[a]	10.10	32
Fst_{seq4} (T)	65	81[a]	8.97	30
Fst_{seq5} (T)	52	63[a]	10.39	31
$TxpA_{seq1}$ (T)	52	84[b]	10.32	35
$TxpA_{seq2}$ (T)	50	82[b]	10.32	35
Type II				
$MazF_{seq}$ (T)	87	93[c]	10.02	120
$MazE_{seq}$ (A)	79	88	4.06	56
$YoeB_{seq1}$ (T)	74	89[d]	9.34	89
$YefM_{seq1}$ (A)	58	77	4.65	88
$YoeB_{seq2}$ (T)	76	86[e]	10.11	88
$YefM_{seq2}$ (A)	68	85	4.31	85

[a] Fst from pSK1 (57).
[b] *S. aureus* N315 TxpA SAS059.
[c] *mazEF*, SACOL2058 and SACOL2059.
[d] *yefM-yoeB*-sa1, SA2195 and SA2196.
[e] *yefM-yoeB*-sa2, SA2245 and SA2246.
[f] Identities and similarities to confirmed (type II) and putative (type I) *S. aureus* homologues (16, 20, 54–57). T, putative toxin; A, putative antitoxin.

degree of similarity to *S. aureus* counterparts was even more pronounced in the case of the putative *mazEF* system (16), as detailed in Fig. 3. An examination of the adjacent genomic context surrounding the candidate *mazEF* genes also revealed an identical gene synteny in *S. equorum* and *S. aureus*. The respective gene pair was hence termed $mazEF_{seq}$ and was further experimentally characterized.

$P_{mazE\ seq}$ lies adjacent to the $mazEF_{seq}$ locus. To provide evidence about the expression of the $mazEF_{seq}$ genes and their transcriptional start point(s), 5′ RACE was conducted using total RNA isolated from exponential-phase *S. equorum* SE3 cells. Sequencing of three independent plasmids containing cDNA from reverse transcription revealed an identical fragment, unambiguously indicating a single transcriptional starting point (TSP) 50 bp upstream of the $mazE_{seq}$ start codon (Fig. 3). Starting at the seventh base preceding the TSP, the sequence $TAGTCA(N)_{17}TATTAT$ was found, likely representing the −35 and −10 sites of a σ^A-dependent promoter separated by a stretch of optimal distance (58). The presumable −35 hexamer was flanked by almost-perfect inverted repeats of the sequence AAAAT(A)GTA, harboring a putative binding site for the *S. aureus* global regulator SarA (59). Starting at the 34th base downstream of the TSP and located eight bases upstream of the start codon, a TGGAGGT stretch represents the probable ribosome-binding site for $mazE_{seq}$. These features reflect almost identical *cis* elements and transcriptional start sites of the orthologous *S. aureus* system (14, 18).

Heterologous overexpression of $MazF_{seq}$ in *E. coli* impairs growth. Tools for the genetic manipulation of *S. equorum* have not been established to date. Therefore, the putative toxin-encoding gene $mazF_{seq}$ was cloned into the tetracycline-inducible *E. coli* cloning vector pASK-IBA3. Induction of $mazF_{seq}$ expression in *E. coli* resulted in an up to 10-fold reduction of OD_{578} values in comparison to those of noninduced strains and those carrying the empty plasmid during the course of the experiment (Fig. 4A). An

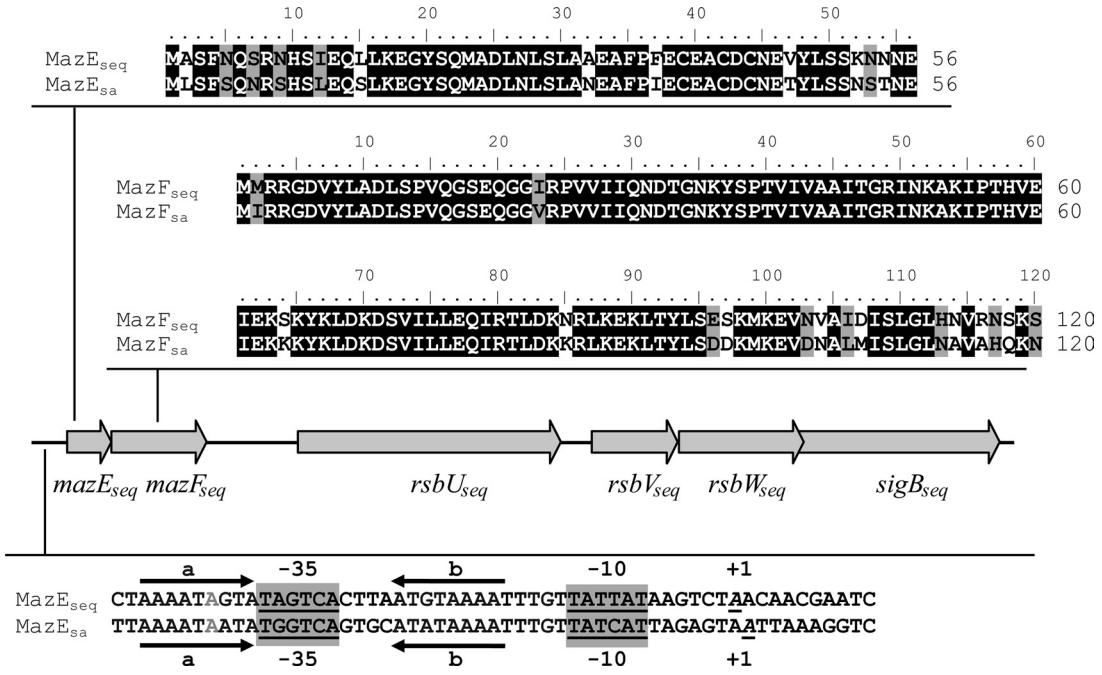

FIG 3 (Top) Alignment of MazF and MazE from *S. equorum* (seq) SE3 with their *S. aureus* (sa) COL homologues (SACOL2058 and SACOL2059). (Middle) Genetic organization of the *mazEF-sigB* locus in *S. equorum* SE3. Gene synteny is identical in *S. aureus* COL (not shown). (Bottom) Transcriptional start point of *mazE* in *S. equorum* SE3 (seq) compared to *S. aureus* COL (sa) (14, 18). Letters "a" and "b" and the corresponding arrows indicate inverted repeats surrounding the −35 region, putatively representing SarA binding sites. Repeat "a" contains a one-base insertion (gray "A") in comparison to repeat "b". "+1" indicates the transcriptional starting point, which is 50 bp upstream of the $mazE_{seq}$ start codon.

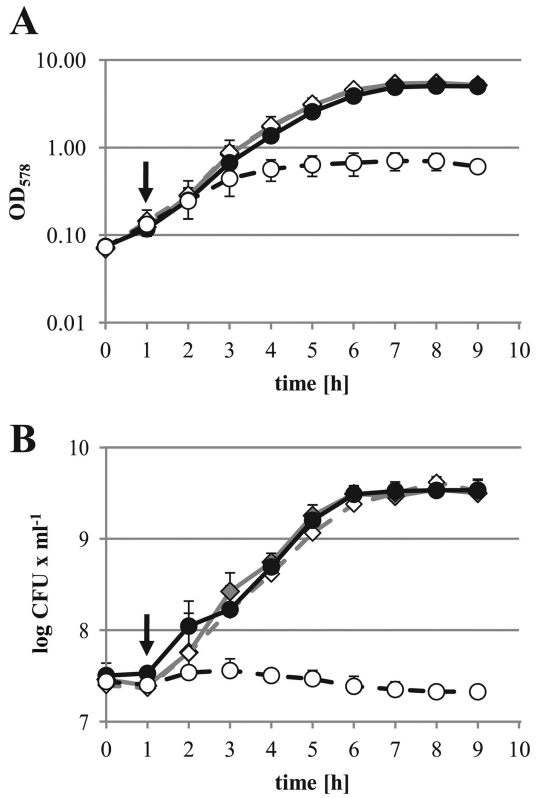

FIG 4 Growth behavior of *E. coli* DH5α(pASK-IBA3) or DH5α(pASK-IBA3 *mazF*$_{seq}$). Induction with 0.4 μM ATc at $t = 1$ h is indicated by arrows. Diamonds connected by solid lines represent growth of *E. coli* DH5α(pASK-IBA3), and circles and dashed lines represent growth of DH5α(pASK-IBA3 *mazF*$_{seq}$). Filled symbols indicate noninduced strains, whereas open symbols denote cultures grown in the presence of ATc. (A) Optical density measurement. (B) CFU analysis.

observation of concomitant CFU values revealed that the expression of MazF$_{seq}$ exerted a bacteriostatic but not a bactericidal effect on *E. coli*, as reflected by rather constant colony counts up to 8 h after induction (Fig. 4B). This observation is in agreement with results from the work of Syed et al. (60), when expression of *Streptococcus mutans mazF* induced growth arrest in *E. coli*. Of note, Fu and colleagues (16) reported bacteriostatic effects upon *mazF*$_{sa}$ overexpression in *S. aureus*. In our experiments, heterologous overexpression of *mazF*$_{seq}$ in *S. aureus* from inducible plasmids did not lead to a growth defect (unpublished results). This was possibly due to cross-interaction of the *S. aureus* antitoxin orthologue with the *S. equorum* toxin or due to weaker expression than that in the previous study, in which a different induction system for *mazF*$_{sa}$ had been used (16).

MazF$_{seq}$ interacts with MazE$_{seq}$ *in vivo*. To check for protein-protein interaction between MazE$_{seq}$ and MazF$_{seq}$, a bacterial two-hybrid analysis using the BACTH system was conducted (41). It makes use of two fragments of adenylate cyclase (T18 and T25) that form an active enzyme only when in close proximity, thus providing evidence for interaction of the fused proteins. Catabolite gene activator protein (CAP)/cAMP-dependent activation of lactose utilization in *E. coli* is visualized by blue colonies on X-Gal-containing medium. Pronounced blue coloring was evident with strains producing MazF$_{seq}$ C terminally fused to the T25 fragment with either N- or C-terminally fused MazE$_{seq}$-T18, suggesting that MazF$_{seq}$ is bound by MazE$_{seq}$ *in vivo* (Fig. 5). This adds to data from the work of Fu et al. (16) demonstrating complex formation of purified MazE$_{sa}$ and MazF$_{sa}$ components *in vitro*. Indeed, the interaction of cognate toxin and antitoxin pairs under nonstress conditions is a characteristic trait of type II TA systems (61), as exemplified by hexameric (MazF$_2$-MazE$_2$-MazF$_2$) complexes in *E. coli* (62). Extensive negative controls yielded colorless colonies, ruling out unspecific β-galactosidase activation observed with the *mazE-mazF* plasmid couples.

MazF$_{seq}$ is a sequence-specific endoribonuclease that preferentially cleaves within the UACAU motif. To determine the catalytic activity and sequence specificity of MazF$_{seq}$, an affinity-purified C-terminally hexahistidine-tagged fusion protein (Fig. 6A) was incubated with 3.5-kb MS2 phage RNA in the presence of CspA *in vitro*, followed by primer extension reactions. In total, seven restriction sites could be determined (Fig. 6B). In five of these cases, UACAU sites were cleaved, mainly after and occasionally before the first uracil. Of note, one out of six UACAU motifs in MS2 RNA appeared to be unaffected (Fig. 6B, C, and D; not all data are shown). In addition, cleavage was observed at the one-base aberrant sequence U/^CCAU, as well

#	T18	T25	Schematic representation (from N to C terminus)
1	-	-	
2	-	Zip	
3	YefM$_{seq}$	MazF$_{seq}$	
4	YefM$_{seq}$	MazF$_{seq}$	
5	MazE$_{seq}$	YoeB$_{seq}$	
6	MazE$_{seq}$	YoeB$_{seq}$	
7	MazE$_{seq}$	MazF$_{seq}$	
8	MazE$_{seq}$	MazF$_{seq}$	
9	Zip	Zip	

FIG 5 Bacterial two-hybrid study to confirm the specific *in vivo* interaction of MazF$_{seq}$ with MazE$_{seq}$. Negative controls (sectors 1 to 6), also including components of the putative YefM-YoeB-seq1 TA system, did not show blue coloration, whereas the leucine zipper positive control (sector 9) yielded colored colonies. Strains BTH101(pUT18-*mazE* pKT25-*mazF*) (sector 7) and BTH101(pUT18C-*mazE* pKT25-*mazF*) (sector 8) showed considerable blue coloration, indicating protein-protein interaction.

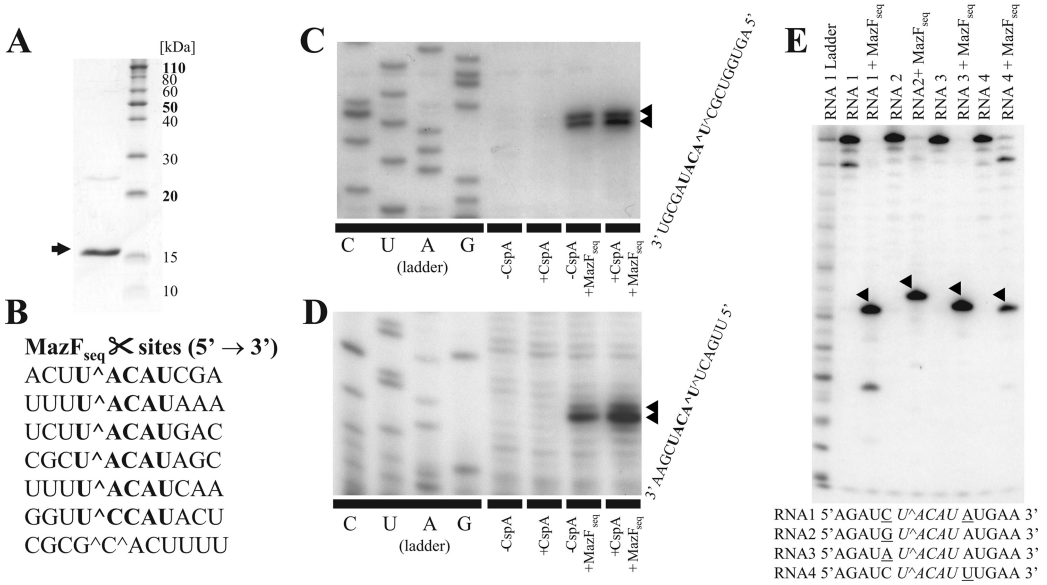

FIG 6 Sequence-specific RNA cleavage of purified MazF$_{seq}$-(His)$_6$. (A) SDS-PAGE of MazF$_{seq}$-(His)$_6$ (15.0 kDa) purified by Ni-NTA affinity chromatography. MazF$_{seq}$-(His)$_6$ protein is indicated by the arrow. (B) Confirmed MazF$_{seq}$-(His)$_6$ target sites in MS2 RNA. (C and D) *In vitro* primer extensions of MS2 phage RNA subjected to MazF$_{seq}$-(His)$_6$ treatment with different radioisotope-labeled primers. In both cases, RNA restriction (arrowheads) was more pronounced in the presence of CspA. Restriction occurred before or after the 5′ uracil of the recognition sequence. Labeling of the sequencing ladder is complementary to the chain terminator dideoxynucleoside triphosphate (ddNTP) used (e.g., ddATP for U lane, etc.). (E) Synthetic RNA oligonucleotides containing the UACAU sequence (preceded and trailed by different bases) were incubated with purified MazF$_{seq}$-(His)$_6$ to verify that the recognition site is confined in length to the pentad sequence UACAU. All four test oligonucleotide RNAs were cut by MazF$_{seq}$-(His)$_6$, with the resulting RNA fragments indicated by arrowheads.

as at CG/\C/\ACU (Fig. 6B). To rule out sequence specificity extending the five-base motif, synthetic RNA oligonucleotides containing UACAU sites flanked by different combinations of bases were treated with MazF$_{seq}$. Restrictions were observed at UACAU sequences preceded by either U or C at the 5′ end and trailed by either C, A, or G at the 3′ end (Fig. 6B). Specific MazF$_{seq}$-dependent restriction in all of these cases suggested that the main MazF$_{seq}$ recognition site is the pentad sequence UACAU, in agreement with the *S. aureus* orthologue (19). Regarding the high degree of similarity between MazF$_{seq}$ and MazF$_{sa}$, this finding is not unexpected; instead, it speaks in favor of UACAU as the major restriction site of both staphylococcal MazF RNA interferases, after an initial report on MazF$_{sa}$ cleavage specificity had reported on a slightly different motif (16). In agreement with studies by Zhu et al. (19, 52), cleavage of some UACAU sites by MazF$_{seq}$ *in vitro* was enhanced in the presence of CspA, evidently due to the removal of higher RNA structures that might impede access of MazF$_{seq}$ to the target site.

We note that the affinity-purified fraction of the MazF$_{seq}$ protein had not been purified to homogeneity (Fig. 6A). To confirm that the RNase activity observed in the *in vitro* primer extension assays was solely conferred by MazF$_{seq}$, *in vivo* primer extensions were conducted. For this, total RNA was extracted from *E. coli* BW25113 cells in which MazF$_{seq}$ had been induced before. Primer extensions were done using the mRNAs of *ompF* and *tufA*, which are confirmed targets for MazF from *Firmicutes* expressed in *E. coli* (50). Judging from respective RNA preparations, defined bands were visible at the UACAU sites directly after the first U in the *in vivo* primer extensions (Fig. 7A and B). These signals were missing in the absence of MazF$_{seq}$, backing up the results from the *in vitro* primer extension assays and suggesting that the specific cleavage of the mRNA is due to the activity of the MazF$_{seq}$ protein.

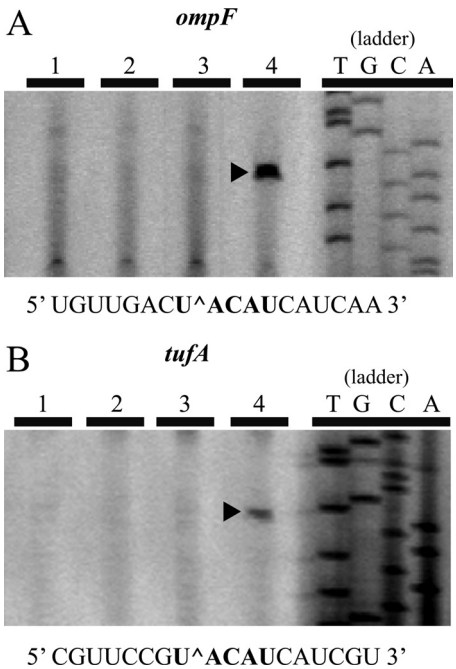

FIG 7 *In vivo* primer extension experiments for MazF$_{seq}$ carried out with different primers (OmpF_ec and TufA_ec) and RNA templates prepared from *E. coli* BW25113 carrying pBAD33 (empty) or carrying pBAD33 SD *mazF$_{seq}$* (*mazF$_{seq}$*). Lanes 1, empty − Ara; lanes 2, empty + Ara; lanes 3, *mazF$_{seq}$* − Ara; lanes 4, *mazF$_{seq}$* + Ara. Reverse transcriptions from the RNA of BW25113 cells with either the empty pBAD33 vector or the uninduced MazF$_{seq}$ construct revealed no cleavage at the UACAU sites, whereas mRNA cleavage at UACAU could be observed in the presence of MazF$_{seq}$ (arrowheads). The result for only one of the two UACAU sites in *tufA* RNA is shown here. The sequencing ladder was done from *E. coli* BW25113 genomic DNA, and the figure inscription represents the bases from the template strand, not the ddNTPs used (e.g., the T lane was created with ddATP etc.).

TABLE 3 Putative $MazF_{seq}$-sensitive CDSs[a]

Locus[b]	*P*	No. of UACAU sites		*L*	Closest *S. aureus* homologue	Putative function
		Actual	Expected			
C3_757	0.99985	6	1.10	612	*sdhC*	Succinate dehydrogenase cytochrome b_{556} subunit
C5_229	0.99976	3	0.29	177		Hypothetical protein
C5_324	0.99967	5	0.90	594		Phospholipase/carboxylesterase
C3_12	0.99964	5	0.91	651	*cysE*	Serine *O*-acetyltransferase
C3_1087	0.99963	6	1.29	570		Heptaprenyl pyrophosphate synthase
C3_700	0.99913	2	0.18	117		Glutaredoxin family
C4_13	0.99899	3	0.43	327	*rsbV*	Anti-sigma B factor antagonist
C5_138	0.99873	8	2.55	1,593	*glvC*	PTS system; arbutin-like IIB component
C5_145	0.99850	6	1.64	1,125		Amidohydrolase family
C3_499	0.99834	3	0.49	348		Hypothetical protein

[a] List of the top 10 putatively $MazF_{seq}$-sensitive coding sequences determined by bioinformatical analysis of the *S. equorum* genome for the occurrence of the sequence UACAU. *P*, probability of UACAU sites as explained in Materials and Methods (used for ranking); *L*, length of the respective gene; PTS, phosphotransferase.
[b] Tentative designation.

Elevated local concentrations of $MazF_{seq}$ target sites in coding sequences. To screen for mRNAs that might be particularly susceptible to $MazF_{seq}$ cleavage in *S. equorum*, a statistical analysis of the occurrences of the UACAU motif in its 2,581 possible CDSs was conducted as previously described (19, 52). According to the equation detailed in Materials and Methods, Table 3 summarizes the top 10 candidate sensitive $MazF_{seq}$ target genes and their closest *S. aureus* orthologues. A number of the putative target CDSs code for hypothetical proteins, whereas the others are likely involved in catabolism of sugars, amino acids, and lipids. Intriguingly, the CDS of *rsbV*, putatively coding for an anti-anti-σ^B factor, might also have a higher susceptibility to $MazF_{seq}$, due to the unusually high abundance of UACAU sites (three copies within 327 bases). Assuming negative regulation of $mazEF_{seq}$ expression by σ^B as in *S. aureus* (14), the conceivable cleavage of *rsbV* by $MazF_{seq}$ would add a coherent second mode of $mazEF_{seq}$ control. As in *S. aureus* (18), a lack of RsbV would arguably result in unbound anti-σ^B factor RsbW, which might thus complex with σ^B. This would abolish the repressive effect of σ^B on $mazEF_{seq}$ expression to impose a positive feedback loop. These assumptions warrant further studies, which may also confirm target genes of $MazF_{seq}$ and unravel the regulation of $mazEF_{seq}$ activity.

Conclusions. To our knowledge, this study describes the first characterization of a putative TA system in a nonpathogenic *Staphylococcus* species. We show that in *S. equorum* SE3, the $mazEF_{seq}$ genes are expressed and are highly similar in sequence, length, position, synteny, and TSP to their *S. aureus* counterparts. Although both the trigger(s) and the function(s) of the MazEF system in *S. equorum* remain enigmatic to date, regulation of staphylococcal pathogenicity, as proposed by Zhu et al. (19), is probably not the sole function of this TA system, which has orthologues in at least seven further *Staphylococcus* species (our unpublished results). In the future, it will be interesting to reveal the instances of activity control, and indeed, besides *sigB S. equorum* also possesses *sarA*, *clpP*, and *clpC* orthologues (unpublished results) possibly involved in regulating $MazE_{seq}$ abundance.

ACKNOWLEDGMENTS

We thank Friedrich Götz for providing access to the raw *S. equorum* SE3 genome and fruitful discussions. Stefan Raue and Daniel Lehle are acknowledged for setting up a GenDB accession platform. We are grateful to Julia Deibert for help with the bacterial two-hybrid experiments.

This work was supported by the Deutsche Forschungsgemeinschaft through grant BE4038/2; by the Wilhelm-Schuler Stiftung, Tübingen; and by a grant from the National Institutes of Health (1R01-GM 081567).

REFERENCES

1. **Leplae R, Geeraerts D, Hallez R, Guglielmini J, Drèze P, Van Melderen L.** 2011. Diversity of bacterial type II toxin-antitoxin systems: a comprehensive search and functional analysis of novel families. Nucleic Acids Res. **39**:5513–5525.
2. **Gerdes K, Christensen SK, Løbner-Olesen A.** 2005. Prokaryotic toxin-antitoxin stress response loci. Nat. Rev. Microbiol. **3**:371–382.
3. **Blower TR, Short FL, Rao F, Mizuguchi K, Pei XY, Fineran PC, Luisi BF, Salmond GPC.** 2012. Identification and classification of bacterial type III toxin-antitoxin systems encoded in chromosomal and plasmid genomes. Nucleic Acids Res. **40**:6158–6173.
4. **Van Melderen L.** 2010. Toxin-antitoxin systems: why so many, what for? Curr. Opin. Microbiol. **13**:781–785.
5. **Fineran PC, Blower TR, Foulds IJ, Humphreys DP, Lilley KS, Salmond GP.** 2009. The phage abortive infection system, ToxIN, functions as a protein-RNA toxin-antitoxin pair. Proc. Natl. Acad. Sci. U. S. A. **106**:894–899.
6. **Masuda H, Tan Q, Awano N, Wu KP, Inouye M.** 2012. YeeU enhances the bundling of cytoskeletal polymers of MreB and FtsZ, antagonizing the CbtA (YeeV) toxicity in *Escherichia coli*. Mol. Microbiol. **84**:979–989.
7. **Wang X, Lord DM, Cheng HY, Osbourne DO, Hong SH, Sanchez-Torres V, Quiroga C, Zheng K, Herrmann T, Peti W, Benedik MJ, Page R, Wood TK.** 2 September 2012. A new type V toxin-antitoxin system where mRNA for toxin GhoT is cleaved by antitoxin GhoS. Nat. Chem. Biol. [Epub ahead of print.] doi:10.1038/nchembio.1062.
8. **Pandey DP, Gerdes K.** 2005. Toxin-antitoxin loci are highly abundant in free-living but lost from host-associated prokaryotes. Nucleic Acids Res. **33**:966–976.
9. **Bukowski M, Rojowska A, Wladyka B.** 2011. Prokaryotic toxin-antitoxin systems—the role in bacterial physiology and application in molecular biology. Acta Biochim. Pol. **58**:1–9.
10. **Mutschler H, Gebhardt M, Shoeman RL, Meinhart A.** 2011. A novel mechanism of programmed cell death in bacteria by toxin-antitoxin systems corrupts peptidoglycan synthesis. PLoS Biol. **9**:e1001033. doi:10.1371/journal.pbio.1001033.
11. **Tan Q, Awano N, Inouye M.** 2011. YeeV is an *Escherichia coli* toxin that inhibits cell division by targeting the cytoskeleton proteins, FtsZ and MreB. Mol. Microbiol. **79**:109–118.
12. **Sayed N, Jousselin A, Felden B.** 2012. A cis-antisense RNA acts in trans in *Staphylococcus aureus* to control translation of a human cytolytic peptide. Nat. Struct. Mol. Biol. **19**:105–112.
13. **Donegan NP, Thompson ET, Fu Z, Cheung AL.** 2010. Proteolytic regulation of toxin-antitoxin systems by ClpPC in *Staphylococcus aureus*. J. Bacteriol. **192**:1416–1422.
14. **Donegan NP, Cheung AL.** 2009. Regulation of the *mazEF* toxin-antitoxin

module in *Staphylococcus aureus* and its impact on *sigB* expression. J. Bacteriol. **191**:2795–2805.
15. **Marianovsky I, Aizenman E, Engelberg-Kulka H, Glaser G.** 2001. The regulation of the *Escherichia coli mazEF* promoter involves an unusual alternating palindrome. J. Biol. Chem. **276**:5975–5984.
16. **Fu Z, Donegan NP, Memmi G, Cheung AL.** 2007. Characterization of MazFSa, an endoribonuclease from *Staphylococcus aureus*. J. Bacteriol. **189**:8871–8879.
17. **Fu Z, Tamber S, Memmi G, Donegan NP, Cheung AL.** 2009. Overexpression of MazFsa in *Staphylococcus aureus* induces bacteriostasis by selectively targeting mRNAs for cleavage. J. Bacteriol. **191**:2051–2059.
18. **Senn MM, Giachino P, Homerova D, Steinhuber A, Strassner J, Kormanec J, Flückiger U, Berger-Bächi B, Bischoff M.** 2005. Molecular analysis and organization of the *sigmaB* operon in *Staphylococcus aureus*. J. Bacteriol. **187**:8006–8019.
19. **Zhu L, Inoue K, Yoshizumi S, Kobayashi H, Zhang Y, Ouyang M, Kato F, Sugai M, Inouye M.** 2009. *Staphylococcus aureus* MazF specifically cleaves a pentad sequence, UACAU, which is unusually abundant in the mRNA for pathogenic adhesive factor SraP. J. Bacteriol. **191**:3248–3255.
20. **Yoshizumi S, Zhang Y, Yamaguchi Y, Chen L, Kreiswirth BN, Inouye M.** 2009. *Staphylococcus aureus* YoeB homologues inhibit translation initiation. J. Bacteriol. **191**:5868–5872.
21. **Ghebremedhin B, Layer F, König W, König B.** 2008. Genetic classification and distinguishing of *Staphylococcus* species based on different partial *gap*, 16S rRNA, *hsp60*, *rpoB*, *sodA*, and *tuf* gene sequences. J. Clin. Microbiol. **46**:1019–1025.
22. **Takahashi T, Satoh I, Kikuchi N.** 1999. Phylogenetic relationships of 38 taxa of the genus *Staphylococcus* based on 16S rRNA gene sequence analysis. Int. J. Syst. Bacteriol. **49**:725–728.
23. **Schleifer K-H, Kilpper-Bälz R, Devriese L.** 1984. *Staphylococcus arlettae* sp. nov., *S. equorum* sp. nov. and *S. kloosii* sp. nov.: three new coagulase-negative, novobiocin-resistant species from animals. Syst. Appl. Microbiol. **5**:501–509.
24. **Carnio MC, Höltzel A, Rudolf M, Henle T, Jung G, Scherer S.** 2000. The macrocyclic peptide antibiotic micrococcin P(1) is secreted by the food-borne bacterium *Staphylococcus equorum* WS 2733 and inhibits *Listeria monocytogenes* on soft cheese. Appl. Environ. Microbiol. **66**: 2378–2384.
25. **Carnio MC, Stachelhaus T, Francis KP, Scherer S.** 2001. Pyridinyl polythiazole class peptide antibiotic micrococcin P1, secreted by food-borne *Staphylococcus equorum* WS2733, is biosynthesized nonribosomally. Eur. J. Biochem. **268**:6390–6401.
26. **Fozo EM, Makarova KS, Shabalina SA, Yutin N, Koonin EV, Storz G.** 2010. Abundance of type I toxin-antitoxin systems in bacteria: searches for new candidates and discovery of novel families. Nucleic Acids Res. **38**: 3743–3759.
27. **Gruber AR, Findeiss S, Washietl S, Hofacker IL, Stadler PF.** 2010. Rnaz 2.0: improved noncoding RNA detection. Pac. Symp. Biocomput. **15**:69–79.
28. **Gruber AR, Neuböck R, Hofacker IL, Washietl S.** 2007. The RNAz web server: prediction of thermodynamically stable and evolutionarily conserved RNA structures. Nucleic Acids Res. **35**:W335–W338.
29. **Larkin MA, Blackshields G, Brown NP, Chenna R, McGettigan PA, McWilliam H, Valentin F, Wallace IM, Wilm A, Lopez R, Thompson JD, Gibson TJ, Higgins DG.** 2007. Clustal W and Clustal X version 2.0. Bioinformatics **23**:2947–2948.
30. **Busch A, Richter AS, Backofen R.** 2008. IntaRNA: efficient prediction of bacterial sRNA targets incorporating target site accessibility and seed regions. Bioinformatics **24**:2849–2856.
31. **Smith C, Heyne S, Richter AS, Will S, Backofen R.** 2010. Freiburg RNA Tools: a web server integrating INTARNA, EXPARNA and LOCARNA. Nucleic Acids Res. **38**:W373–W377.
32. **Benham CJ, Bi C.** 2004. The analysis of stress-induced duplex destabilization in long genomic DNA sequences. J. Comput. Biol. **11**:519–543.
33. **Herbig A, Nieselt K.** 2011. nocoRNAc: characterization of non-coding RNAs in prokaryotes. BMC Bioinformatics **12**:40. doi:10.1186/1471-2105-12-40.
34. **Sevin EW, Barloy-Hubler F.** 2007. RASTA-Bacteria: a web-based tool for identifying toxin-antitoxin loci in prokaryotes. Genome Biol. **8**:R155. doi: 10.1186/gb-2007-8-8-r155.
35. **Shao Y, Harrison EM, Bi D, Tai C, He X, Ou HY, Rajakumar K, Deng Z.** 2011. TADB: a web-based resource for type 2 toxin-antitoxin loci in bacteria and archaea. Nucleic Acids Res. **39**:D606–D611.
36. **Waterhouse AM, Procter JB, Martin DM, Clamp M, Barton GJ.** 2009. Jalview version 2—a multiple sequence alignment editor and analysis workbench. Bioinformatics **25**:1189–1191.
37. **Hall TA.** 1999. BioEdit: a user-friendly biological sequence alignment editor and analysis program for Windows 95/98/NT. Nucleic Acids Symp. Ser. **41**:95–98.
38. **Studier FW, Moffatt BA.** 1986. Use of bacteriophage T7 RNA polymerase to direct selective high-level expression of cloned genes. J. Mol. Biol. **189**: 113–130.
39. **Hanahan D.** 1985. DNA cloning 1: a practical approach. IRL Press, McLean, VA.
40. **Baba T, Ara T, Hasegawa M, Takai Y, Okumura Y, Baba M, Datsenko KA, Tomita M, Wanner BL, Mori H.** 2006. Construction of *Escherichia coli* K-12 in-frame, single-gene knockout mutants: the Keio collection. Mol. Syst. Biol. **2**:2006.0008. doi:10.1038/msb4100050.
41. **Karimova G, Pidoux J, Ullmann A, Ladant D.** 1998. A bacterial two-hybrid system based on a reconstituted signal transduction pathway. Proc. Natl. Acad. Sci. U. S. A. **95**:5752–5756.
42. **Guzman LM, Belin D, Carson MJ, Beckwith J.** 1995. Tight regulation, modulation, and high-level expression by vectors containing the arabinose P_{BAD} promoter. J. Bacteriol. **177**:4121–4130.
43. **Qing G, Ma LC, Khorchid A, Swapna GV, Mal TK, Takayama MM, Xia B, Phadtare S, Ke H, Acton T, Montelione GT, Ikura M, Inouye M.** 2004. Cold-shock induced high-yield protein production in *Escherichia coli*. Nat. Biotechnol. **22**:877–882.
44. **Smith HO, Levine M.** 1964. Two sequential repressions of DNA synthesis in the establishment of lysogeny by phage P22 and its mutants. Proc. Natl. Acad. Sci. U. S. A. **52**:356–363.
45. **Bera A, Herbert S, Jakob A, Vollmer W, Götz F.** 2005. Why are pathogenic staphylococci so lysozyme resistant? The peptidoglycan *O*-acetyltransferase OatA is the major determinant for lysozyme resistance of *Staphylococcus aureus*. Mol. Microbiol. **55**:778–787.
46. **Hanahan D.** 1983. Studies on transformation of *Escherichia coli* with plasmids. J. Mol. Biol. **166**:557–580.
47. **Albrecht T, Raue S, Rosenstein R, Nieselt K, Götz F.** 2012. Phylogeny of the staphylococcal major autolysin and its use in genus and species typing. J. Bacteriol. **194**:2630–2636.
48. **Marmur J.** 1961. A procedure for the isolation of deoxyribonucleic acid from micro-organisms. J. Mol. Biol. **3**:208–218.
49. **Chatterjee S, Jiang W, Emerson SD, Inouye M.** 1993. The backbone structure of the major cold-shock protein CS7.4 of *Escherichia coli* in solution includes extensive β-sheet structure. J. Biochem. **114**:663–669.
50. **Rothenbacher FP, Suzuki M, Hurley JM, Montville TJ, Kirn TJ, Ouyang M, Woychik NA.** 2012. *Clostridium difficile* MazF toxin exhibits selective, not global, mRNA cleavage. J. Bacteriol. **194**:3464–3474.
51. **Halfmann A, Hakenbeck R, Brückner R.** 2007. A new integrative reporter plasmid for *Streptococcus pneumoniae*. FEMS Microbiol. Lett. **268**: 217–224.
52. **Zhu L, Phadtare S, Nariya H, Ouyang M, Husson RN, Inouye M.** 2008. The mRNA interferases, MazF-mt3 and MazF-mt7 from *Mycobacterium tuberculosis* target unique pentad sequences in single-stranded RNA. Mol. Microbiol. **69**:559–569.
53. **Meyer F, Goesmann A, McHardy AC, Bartels D, Bekel T, Clausen J, Kalinowski J, Linke B, Rupp O, Giegerich R, Pühler A.** 2003. GenDB—an open source genome annotation system for prokaryote genomes. Nucleic Acids Res. **31**:2187–2195.
54. **Kwong SM, Jensen SO, Firth N.** 2010. Prevalence of Fst-like toxin-antitoxin systems. Microbiology **156**:975–977.
55. **Weaver KE, Reddy SG, Brinkman CL, Patel S, Bayles KW, Endres JL.** 2009. Identification and characterization of a family of toxin-antitoxin systems related to the *Enterococcus faecalis* plasmid pAD1 par addiction module. Microbiology **155**:2930–2940.
56. **Beaume M, Hernandez D, Farinelli L, Deluen C, Linder P, Gaspin C, Romby P, Schrenzel J, Francois P.** 2010. Cartography of methicillin-resistant *S. aureus* transcripts: detection, orientation and temporal expression during growth phase and stress conditions. PLoS One **5**:e10725. doi: 10.1371/journal.pone.0010725.
57. **Jensen SO, Apisiridej S, Kwong SM, Yang YH, Skurray RA, Firth N.** 2010. Analysis of the prototypical *Staphylococcus aureus* multiresistance plasmid pSK1. Plasmid **64**:135–142.

58. **Helmann JD.** 1995. Compilation and analysis of *Bacillus subtilis sigma A*-dependent promoter sequences: evidence for extended contact between RNA polymerase and upstream promoter DNA. Nucleic Acids Res. **23**: 2351–2360.
59. **Chien Y-T, Manna AC, Projan SJ, Cheung AL.** 1999. SarA, a global regulator of virulence determinants in *Staphylococcus aureus*, binds to a conserved motif essential for *sar*-dependent gene regulation. J. Biol. Chem. **274**:37169–37176.
60. **Syed MA, Koyanagi S, Sharma E, Jobin MC, Yakunin AF, Lévesque CM.** 2011. The chromosomal *mazEF* locus of *Streptococcus mutans* encodes a functional type II toxin-antitoxin addiction system. J. Bacteriol. **193**: 1122–1130.
61. **Yamaguchi Y, Inouye M.** 2011. Regulation of growth and death in *Escherichia coli* by toxin-antitoxin systems. Nat. Rev. Microbiol. **9**:779–790.
62. **Kamada K, Hanaoka F, Burley SK.** 2003. Crystal structure of the MazE/MazF complex: molecular bases of antidote-toxin recognition. Mol. Cell **11**:875–884.
63. **Katoh K, Kuma K, Miyata T, Toh H.** 2005. Improvement in the accuracy of multiple sequence alignment program MAFFT. Genome Inform. **16**(1): 22–33.